

RESEARCH

Open Access



# Metformin exerted tumoricidal effects on colon cancer tumoroids via the regulation of autophagy pathway

Roya Shabkhizan<sup>1,2</sup>, Çiğır Biray Avci<sup>3</sup>, Sanya Haiaty<sup>1</sup>, Marziyeh Sadat Moslehian<sup>1,2</sup>, Fatemeh Sadeghsoltani<sup>4</sup>, Ahad Bazmani<sup>1</sup>, Mahdi Mahdipour<sup>5</sup>, Leila Sabour Takanlou<sup>3</sup>, Maryam Sabour Takanlou<sup>3</sup>, Arezoo Rezaie Nezhad Zamani<sup>5</sup> and Reza Rahbarghazi<sup>5,6\*</sup> 

## Abstract

**Background** Despite the existence of promising outcomes from standard 2D culture systems, these data are not completely akin to in vivo tumor parenchyma. Therefore, the development and fabrication of various 3D culture systems can in part mimic intricate cell-to-cell interaction within the real tumor mass. Here, we aimed to evaluate the tumoricidal impacts of metformin (MTF) on colorectal cancer (CRC) tumoroids in an in vitro system via the modulation of autophagy.

**Methods** CRC tumoroids were developed using human umbilical vein endothelial cells (HUVECs), adenocarcinoma HT29 cells, and fibroblasts (HFFF2) in a ratio of 1: 2: 1 and 2.5% methylcellulose. Tumoroids were exposed to different concentrations of MTF, ranging from 20 to 1000 mM, for 72 h. The survival rate was detected using an LDH release assay. The expression and protein levels of autophagy-related factors were measured using PCR array and western blotting, respectively. Using H & E, and immunofluorescence staining (Ki-67), the integrity and proliferation rate of CRC tumoroids were examined.

**Results** The current protocol yielded typical compact tumoroids with a dark central region. Despite slight changes in released LDH contents, no statistically significant differences were achieved in terms of cell toxicity in MTF-exposed groups compared to the control tumoroids, indicating the insufficiency of MTF in the induction of tumor cell death ( $p > 0.05$ ). Western blotting indicated that the LC3II/I ratio was reduced in tumoroids exposed to 120 mM MTF ( $p < 0.05$ ). These data coincided with the reduction of intracellular p62 content in MTF 120 mM-treated tumoroids compared to MTF 40 mM and control groups ( $p < 0.05$ ). PCR array analysis confirmed the up-regulation, and down-regulation of several genes related to various signaling transduction pathways associated with autophagy machinery and shared effectors between autophagy and apoptosis in 40 and 120 mM MTF groups compared to the non-treated control group ( $p < 0.05$ ). These changes were more prominent in tumoroids incubated with 120 mM MTF. Histological examination confirmed the loosening integrity of tumoroids in MTF-treated groups, especially 120 mM MTF, with the increase in cell death via the induction of apoptosis (chromatin marginalization) and necrotic (pyknotic nuclei) changes. In the 120 mM MTF group, spindle-shaped cells with the remnants of a fibrillar matrix were detected. Data indicated the reduction of proliferating Ki-67<sup>+</sup> cells within the tumoroids by increasing the MTF concentration from 40 to 120 mM.

\*Correspondence:

Reza Rahbarghazi

rezarahbardvm@gmail.com; rahbarghazir@tbzmed.ac.ir

Full list of author information is available at the end of the article



© The Author(s) 2025. **Open Access** This article is licensed under a Creative Commons Attribution-NonCommercial-NoDerivatives 4.0 International License, which permits any non-commercial use, sharing, distribution and reproduction in any medium or format, as long as you give appropriate credit to the original author(s) and the source, provide a link to the Creative Commons licence, and indicate if you modified the licensed material. You do not have permission under this licence to share adapted material derived from this article or parts of it. The images or other third party material in this article are included in the article's Creative Commons licence, unless indicated otherwise in a credit line to the material. If material is not included in the article's Creative Commons licence and your intended use is not permitted by statutory regulation or exceeds the permitted use, you will need to obtain permission directly from the copyright holder. To view a copy of this licence, visit <http://creativecommons.org/licenses/by-nc-nd/4.0/>.

**Conclusions** Different shared autophagy/apoptosis genes were modulated in CRC tumoroids after MTF treatment coinciding with both typical necrotic and apoptotic cells within the tumoroid structure. MTF can inhibit the integrity and proliferation of CRC tumoroids in dose-dependent manner.

**Keywords** Colorectal adenocarcinoma cancer, Tumoroids, Metformin, Autophagy, Apoptosis, Tumoricidal effects

## Introduction

Colorectal cancers (CRCs) are the most debilitating pathological conditions of the gastrointestinal tract with high-rate morbidities and mortalities in clinical settings [1]. To date, several attempts have been made to find appropriate therapeutics in cancer patients to reduce the progression of CRC development to the remote sites. Unfortunately, most therapeutic strategies are not effective enough and cause side effects. Therefore, novel therapeutic approaches should be developed to circumvent the failure of medication protocols [2]. Unfortunately, most conventional therapeutic regimes have been examined in 2D culture systems that could not reflect completely in vivo-like conditions described within the tumor niche [3]. The direct in vitro incubation of monolayer cells in the 2D culture systems to the chemotherapeutics can contribute to rapid cancer cell atresia in doses less than those of in vivo conditions [4]. Because of physical stromal barriers and stiffened extracellular matrix (ECM) within the tumor parenchyma, finding the actual tumoricidal doses is problematic [5].

In recent years, the advent and development of sophisticated culture systems, especially spheroids/organoids are helpful to overcome the limitations of 2D culture systems [3, 6]. Organoids/spheroids can in part but not completely mimic in vivo-like conditions with juxtaposed several cell types compared to conventional culture systems [7, 8]. Even though, the incubation of patient-derived tumor organoids, known also tumoroids, with chemotherapeutics is a high-throughput drug screening platform in each cancer case [9]. Histological examinations have shown that there are similarities between spheroids/organoids with human natural tumors in terms of necrotic and proliferative regions, and certain signaling pathways [10–13].

Autophagy is an early-stage cell response against external stimuli and insulting conditions [14]. The activation of autophagy has been shown to help CRC cells escape stressful conditions by the restoration of injured organelles and misfolded proteins [15]. Autophagy consists of multiple effectors such as mammalian target of rapamycin (mTOR) and autophagy-related genes (ATGs). The sequential activation of ATGs can lead to the formation of double-membrane autophagosomes. The fusion of autophagosomes with lysosomes contributes to the formation of autophagolysosomes and the

elimination of injured organelles and misfolded biomolecules [16]. However, the overactivation of autophagy can increase the degradation of subcellular components and thus sensitize the cells to death under stressful conditions [17]. These data indicate that autophagy functions as a double-edged sword in terms of cell survival and dynamic growth [18].

It has been shown that metformin (MTF) can reduce the dynamic growth of tumor cells via the regulation of mTOR in AMP-activated protein kinase (AMPK)-dependent and independent manners [19]. In response to MTF administration, the systemic levels of insulin and insulin-like growth factor-1 are reduced which can per se diminish the cancer cell proliferation and expansion [19]. In terms of CRCs, several studies have examined the relationship between the MTF administration and the probability of CRC development with conflicting results [20–30]. Most of the data have been obtained from the effect of MTF on cancer cells in 2D culture systems and animal models. To the best of our knowledge, there are few reports targeting the tumoricidal effects of MTF on 3D CRC tumoroids. Here, 3D CRC tumoroids were established using different three-cell lines, including human colorectal adenocarcinoma HT-29 cells, fetal foreskin fibroblasts (HFFF2 cells), and human umbilical vein endothelial cells (HUVECs) and exposed to different doses of MTF for 72 h. The survival rate, tumoroid integrity, and autophagy response were monitored in in vitro conditions. Data from the present study can help us understand the underlying tumoricidal properties of MTF in the CRC tumoroid system.

## Methods

### Cell culture protocol

Human HT-29, HFFF2 cells, and HUVECs were purchased from the Iranian National Cell Bank (Pasture institute, Tehran). The cells were cultured in RPMI-1640 medium (Cat no; 21,875–034; Gibco) with 10% fetal bovine serum (FBS; Cat no; 26140–079; Gibco) and 1% Pen-Strep (Cat no; 10,378–016; Gibco) under standard conditions. To subculture the cells, 0.25% Trypsin–EDTA (Cat no; R001100; Gibco) solution was used. Cells that were used at passages 3–6 after reaching 70–80% confluence for different analyses.

### CRC tumoroid formation

CRC tumoroids were developed using the hanging drop technique as previously described by our research group [3]. CRC tumoroids with a total cell number of  $1 \times 10^3$  were developed using HT-29, HFFF2, and HUVECs at a ratio of 2:1:1, respectively in a culture medium (25  $\mu$ l) containing 1% FBS and 2.5% methylcellulose (Cat no: MO512; Sigma-Aldrich). The mixture of cells was carefully placed into the inner surface of a 10 cm culture dish lid (SPL) and kept in standard conditions for 72 h. To avoid the culture medium evaporation, the bottom surface of the plates was filled with sterile phosphate-buffered saline (PBS) solution.

### Cytotoxicity test

Tumoroids were gently transferred onto each well of 96-well plates and exposed to different doses of MTF, 20, 40, 60, 80, 200, 400, 600, 800, and 1000 mM. After 72 h, released lactate dehydrogenase (LDH) contents were measured in supernatants using LDH Cytotoxicity Assay kits (Pars Azmun Co. Ltd, Iran) at a wavelength of 340 nm. In the current experiment, MTF at doses of 40 and 120 mM was used for subsequent analyses according to the previously published data [31].

### Tumoroids size and integrity

The integrity of CRC tumoroids was assessed 72 h after being treated with 40 and 120 mM MTF using bright-field microscopy and ImageJ software (NIH, Ver. 1.4). The data in MTF-treated groups were compared to the non-treated control tumoroids.

### Western blotting analysis

Protein levels of autophagy factors, including Beclin-1, LC3, and p62 were measured using western blotting in MTF-treated and control tumoroids. After a 72-h incubation period, tumoroids were lysed using lysis buffer, and centrifuged at 14,000 rpm for 20 min. Protein samples were loaded and electrophoresed at 10% SDS-PAGE gel and transferred onto the PVDF membrane. Following blocking 1% skim milk for one hour, membranes were incubated with antibodies against target proteins [Beclin-1 (Cat no: sc-48341 Santa Cruz Biotechnology, Inc), LC3 (Cat no: Cell Signaling Technology, Inc) and p62 (Cat no: sc-10117 Santa Cruz Biotechnology, Inc)] at 4°C overnight. The membranes were washed three times with PBST solution and incubated with an HRP-conjugated secondary antibody (Cat no: sc-2357 Santa Cruz Biotechnology, Inc) to label the immunoblots. The reactive bands were detected using X-ray films and ECL solution. Immunoreactive bands were semi-quantitatively scored using ImageJ software (NIH) related to  $\beta$ -actin (Cat no: sc-47778 Santa Cruz Biotechnology, Inc).

### PCR array analysis

The expression of various autophagy mediators was quantitated using PCR array analysis (Supplementary Table 1). Total RNA of CRC tumoroids was extracted using the Trizol Reagent RNA extraction kit (Cat no: 302-001; RiboExLs) after being exposed to 40 and 120 mM MTF for 72 h. Takara cDNA Synthesis Kit (Cat no: RR037A) was used to reverse-transcribed the isolated RNAs. Transcription levels were monitored using Human Autophagy RT2 Profiler PCR Array (Cat no: PAHS-084Z; Qiagen GeneGlobe), and Light Cycler 480 Instrument II (Roche) using  $2^{-\Delta\Delta CT}$  formula. In this study, transcription rates exceeding a twofold increase were considered as the threshold value based on the results of three experimental trials.

### Hematoxylin–eosin (H & E) staining

CRC tumoroids were stained with H & E solution after being exposed to 40 and 120 mM MTF. To preserve the integrity and prevent any artifact effects, the treated CRC tumoroids were incubated in 1% agar solution and allowed to solidify. Samples were fixed with 10% buffered formalin solution, dehydrated, and 5  $\mu$ m thick sections were prepared. Using the H & E solution, the samples were imaged and data were compared to the control group.

### Immunofluorescence assay

To monitor whether MTF treatment can alter the proliferation of CRC tumoroids, immunofluorescence (IF) staining of nuclear Ki-67 was performed. To this end, 5  $\mu$ m thick sections were permeabilized with 0.1% Triton-X100 solution for 5 min, washed with PBS, and blocked using 1% bovine serum albumin (Sigma-Aldrich) for 30 min at room temperature. After that, samples were incubated with anti-human Ki-67 antibody (Santa Cruz Biotechnology Inc.) for 1 h at room temperature. The process was continued with three-time PBS washes and incubation with FITC-conjugated secondary antibody (Santa Cruz Biotechnology Inc.) for 30–60 min. In the next step, the slides were washed with PBS and 1  $\mu$ g/ml DAPI solution was used for counterstaining.

### Statistical analysis

Data (Mean  $\pm$  SD) were analyzed in the Prism 5.0 (GraphPad) software using a One-way ANOVA with the Tukey post hoc Multiple Comparison Test.  $p < 0.05$  was considered statistically significant.

## Results

### Tumoroid morphology

In this study, an in vitro 3D CRC tumoroid was developed using the hanging drop method to evaluate the

tumoricidal properties of MTF after 72 h. According to bright-field images, CRC tumoroids showed a center dark zone enclosed by a relatively bright peripheral area (outer layer). The outer layer consists of numerous proliferating round cells and flattened spindle cells at the external surface (Fig. 1A). These data show the efficiency of our protocol in the development of CRC tumoroids consisting of three cell lineages including HT-29, HFFF2 cells, and HUVECs.

**MTF did not influence the survival rate of CRC tumoroids**

The viability of MTF-treated CRC tumoroids was determined using an LDH release assay after being exposed to different doses of MTF, ranging from 20 to 1000 mM (Fig. 1B). Data indicated the lack of significant cytotoxicity of MTF on CRC tumoroids related to the control group after 72 h ( $p > 0.05$ ; Fig. 1B). Despite the slight reduction of released LDH content in 1000 mM MTF, these values did not reach statistically significant levels

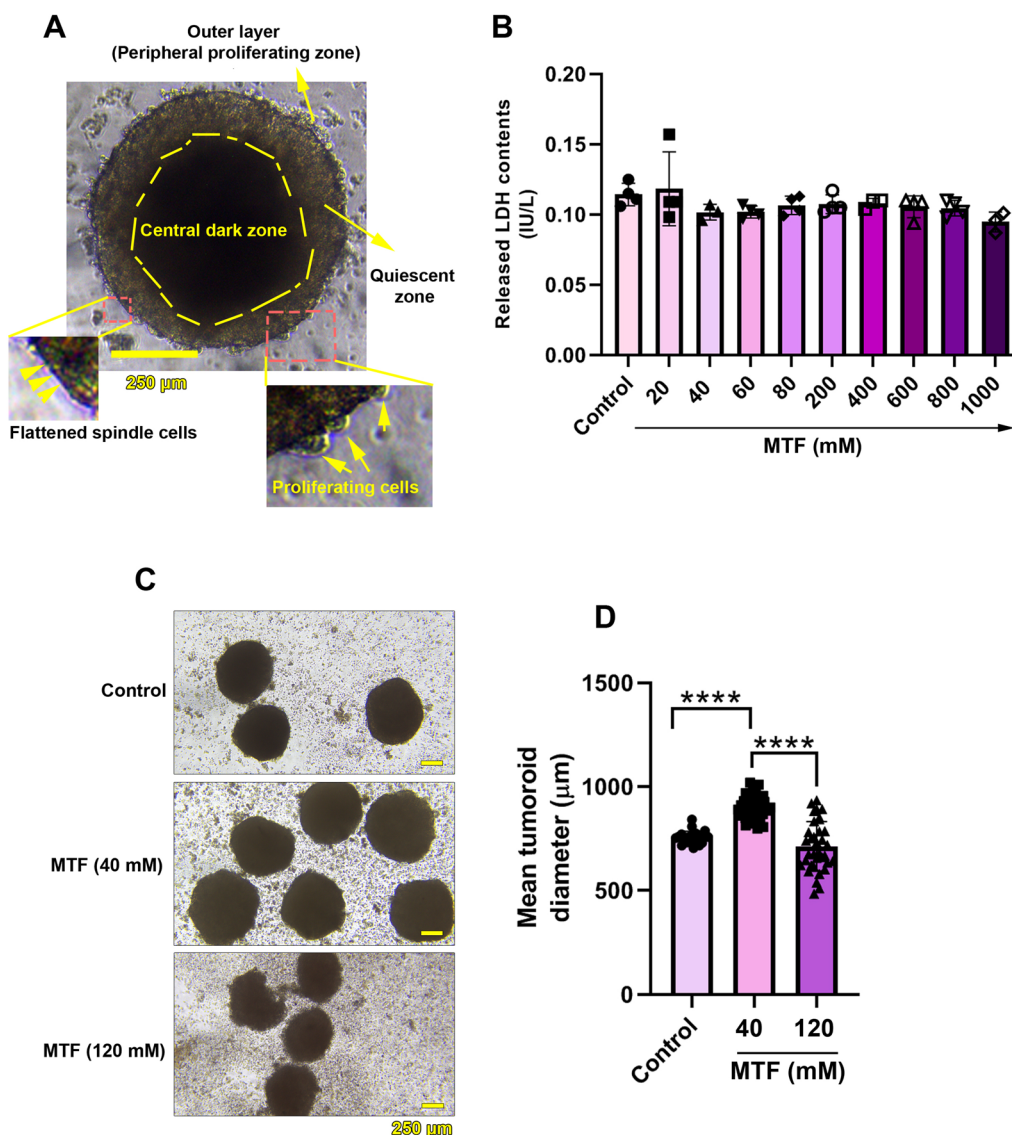


**Fig. 1** Typical CRC tumoroid structure developed using three cell lines, including HT-29, HFFF2 cells, and HUVECs at the ratio of 2: 1: 1. Three distinct layers, central dark, quiescent, and outermost regions can be detected in CRC tumoroids (A). Analyzing the viability of cells within the CRC tumoroids after being exposed to different doses of MTF (20, 40, 60, 80, 200, 400, 600, 800, and 1000 mM) for 72 h (B;  $n = 4$ ). Data indicated the lack of significant data between the MTF-treated tumoroids and the control group ( $p = 0.2460$ ;  $df = 27$ ). Monitoring mean CRC tumoroid diameter after being exposed to 40 and 120 mM MTF in 10 randomly selected microscopic fields compared to the control group (C and D). Incubation of CRC tumoroids with 40 mM MTF led to an increase in mean size compared to control and 120 mM MTF-treated tumoroids ( $p_{\text{Control vs. 40 } \mu\text{M}} < 0.0001$ ;  $p_{\text{Control vs. 120 } \mu\text{M}} = 0.1367$ ;  $p_{40 \mu\text{M vs. 120 } \mu\text{M}} < 0.0001$ ). One-way ANOVA with Tukey post hoc analysis. \*\*\*\* $p < 0.0001$

( $p > 0.05$ ). Based on the results, increasing doses of MTF cannot affect the survival rate of cells within the CRC tumoroids in in vitro conditions.

**MTF influenced CRC tumoroid size**

Based on the LDH release assay, 40 and 120 mM MTF were selected for subsequent analyses (Fig. 1C-D). We noted that the mean CRC tumoroids diameter was increased in the 40 mM MTF group compared to the non-treated control CRC tumoroids ( $p < 0.0001$ ). By increasing the MTF concentration to 120 mM, the size of CRC tumoroids was close to the size of control tumoroids ( $p > 0.05$ ). Similarly, the size of tumoroids

was increased in the 40 mM MTF as compared to the 120 mM MTF group ( $p < 0.0001$ ). Bright-field data confirmed the existence of numerous single cells and small cell aggregates on the surface of the culture plate in the 120 mM MTF group. This effect would be associated with the tumoricidal effects of MTF leading to surface cell disaggregation.

**MTF stimulated autophagy response in CRC tumoroids**

To assess whether 40 and 120 mM MTF can regulate the autophagy response in CRC tumoroids, protein levels of Beclin-1, LC3, and p62 were assessed using western blotting (Fig. 2). Data indicated that protein levels

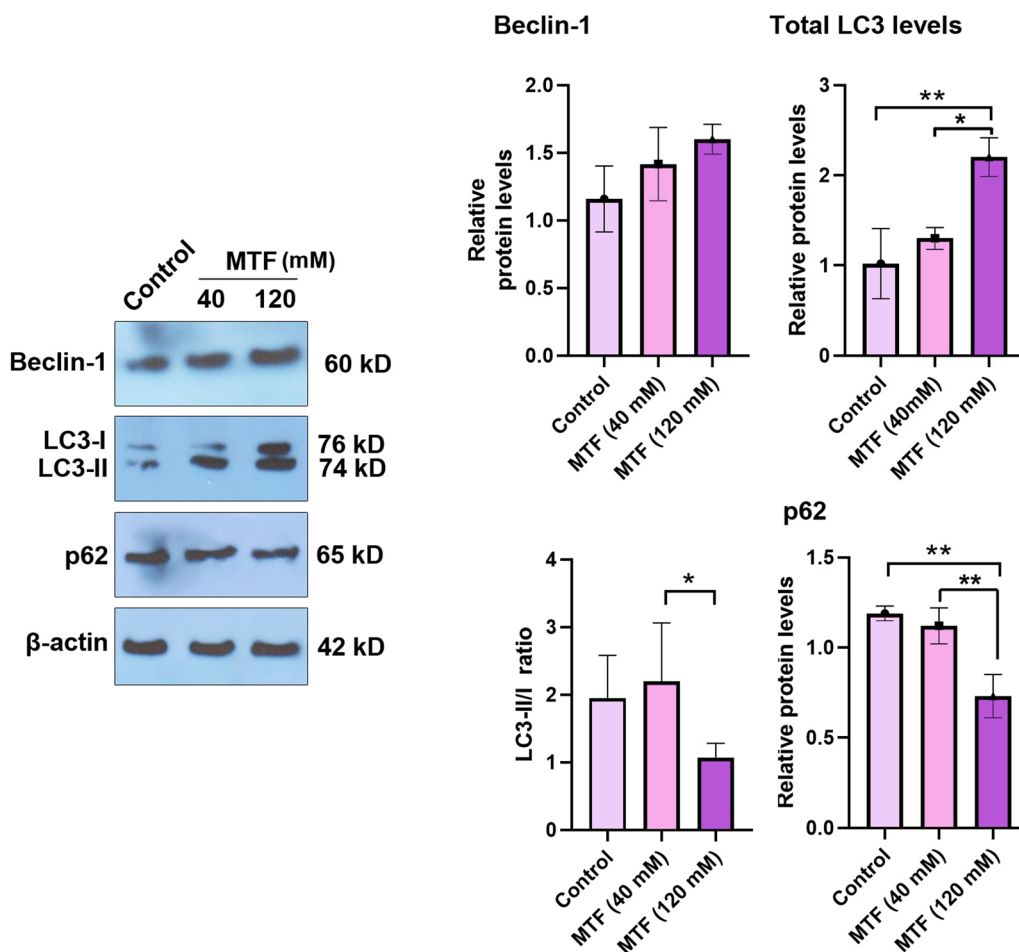


**Fig. 2** Western blot analysis of autophagy-related mediators (Beclin-1, total LC3, LC3-II/I ratio, and p62) in CRC tumoroids after treatment with 40 and 120 mM MTF for 72 h. Samples were pooled from three separate replicates for each blot (total  $n = 6$ ). Data indicated the lack of significant differences in protein levels of Beclin-1 ( $p_{\text{Control vs. MTF (40 mM)}} = 0.3866$ ;  $p_{\text{Control vs. MTF (120 mM)}} = 0.1085$ ;  $p_{\text{MTF (40 mM) vs. MTF (120 mM)}} = 0.5895$ ;  $df = 6$ ). The incubation of tumoroids with MTF led to a significant increase of total LC3 in 120 mM MTF compared to the control group ( $p_{\text{Control vs. MTF (40 mM)}} = 0.4516$ ;  $p_{\text{MTF (40 mM) vs. MTF (120 mM)}} = 0.0144$ ;  $p_{\text{Control vs. MTF (120 mM)}} = 0.0039$ ;  $df = 6$ ). Along with these changes, the LC3-II/I was reduced in 120 mM MTF-treated tumoroids compared to the 40 mM MTF-treated group ( $p_{\text{Control vs. MTF (40 mM)}} = 0.7727$ ;  $p_{\text{Control vs. MTF (120 mM)}} = 0.0684$ ;  $p_{\text{MTF (40 mM) vs. MTF (120 mM)}} = 0.0181$ ;  $df = 15$ ). The levels of p62 were reduced in 120 mM MTF groups compared to 40 mM MTF-treated and control groups ( $p_{\text{Control vs. MTF (40 mM)}} = 0.6481$ ;  $p_{\text{Control vs. MTF (120 mM)}} = 0.0022$ ;  $p_{\text{MTF (40 mM) vs. MTF (120 mM)}} = 0.0052$ ;  $df = 6$ ). One-way ANOVA with Tukey post hoc test. \*\* $p < 0.01$ ; \*\*\* $p < 0.001$ , \*\*\*\* $p < 0.0001$

of Beclin-1 were slightly increased by changing the concentration of MTF from 40 to 120 mM. However, these values did not reach significant levels compared to the control group ( $p > 0.05$ ; Fig. 2). It was noted that total levels of LC3 were significantly increased in the 120 mM MTF group compared to 40 mM MTF-treated ( $p < 0.05$ ) and control tumoroids ( $p < 0.01$ ). Of note, the treatment of CRC tumoroids with MTF at a dose of 120 mM led to a significant reduction of the LC3-II/I ratio, indicating the inhibition of autophagy flux ( $p > 0.05$ ; Fig. 2). There is no significant difference related to the LC3-II/I ratio between the control and 40 mM MTF groups. Along with these changes, the intracellular levels of p62 were diminished only in the 120 mM MTF group compared to the non-treated tumoroids ( $p < 0.05$ ; Fig. 2). These data demonstrate that MTF can influence the autophagy status in CRC tumoroids in higher doses.

#### MTF altered the expression of autophagy-related genes

To evaluate the gene expression of the autophagy signaling pathway genes, a PCR array analysis was conducted (Table 1, Fig. 3, and Supplementary Fig. 1). The volcano plot revealed the identification of significant changes in gene expression across treatment conditions. The results showed the changes in the expression of various genes in 40 and 120 mM MTF groups after 72 h. Data showed that the expression of genes related to vacuole formation, ATG4A (13.42-fold and 23.82-fold), ATG4B (3.31-fold and 6.25-fold), ATG9A (14.99-fold and 44.14-fold), IRGM (21.35-fold and 8.08-fold), MAP1LC3A (26.83-fold and 12.41-fold), MAP1LC3B (9.62-fold and 15.71-fold), ULK1 (732.15-fold and 767.49-fold), WIPI1 (32.36-fold and 68.31-fold) were up-regulated in 40 and 120 mM MTF groups compared to control tumoroids, respectively. ATG4D (-2.08-fold and -3.52-fold), and BECN1 (-2.21-fold and -4.49-fold) were also down-regulated in doses of 40 and 120 mM MTF, respectively. Based on our data, ATG12 exhibited a strong down-regulation in the 120 mM MTF group (-64,009.57-fold) compared to CRC tumoroids exposed to 40 mM MTF (15.1-fold). Changes in the expression of ATG4C (4.68-fold), ATG5 (2.36-fold), RGS19 (7.6-fold) were observed in the dose of 40 mM and AMBRA1 (-3.42), GABARAP (2.49-fold) at the dose of 120 mM MTF. Genes such as ATG4A, B, C, D, and GABARAP are involved in vacuole targeting and protein transport signaling transduction pathways. Of note, 40 and 120 mM MTF altered the expression of genes ATG9A, ATG10 (4.46-fold and 6.89-fold), ATG16L2 (7945.93-fold and 26,140.52-fold), ATG3 (6.17-fold and 3.57-fold), and RAB24 (-2.47-fold and -2.63-fold) compared to the control group. It was suggested that ATG4A, B, C, and D mediators exhibit proteolytic activity and can affect the autophagy flux through their interaction with

**Table 1** PCR array analysis of human autophagy signaling pathway in CRC tumoroids treated with 40 and 120 mM MTF for 72 h

Gene	Met (40)	Met (120)	Gene	Met (40)	Met (120)
<i>AKT1</i>	4.33	6.16	<i>GABARAPL2</i>	-1.30	-1.56
<i>AMBRA1</i>	-1.07	-3.42	<i>HDAC1</i>	-1.25	256.71
<i>APP</i>	26.46	77.92	<i>HDAC6</i>	5.60	7.03
<i>ATG10</i>	4.46	6.89	<i>HGS</i>	-1.13	-72,014.51
<i>ATG12</i>	15.10	-64,009.57	<i>HSP90AA1</i>	-1.25	531.53
<i>ATG16L1</i>	1.43	1.95	<i>HSPA8</i>	4.65	2.94
<i>ATG16L2</i>	7945.93	26,140.52	<i>HTT</i>	6.00	4.84
<i>ATG3</i>	6.17	3.57	<i>IFNG</i>	243,911.80	-2.42
<i>ATG4A</i>	13.42	23.82	<i>IGF1</i>	2.69	-5.05
<i>ATG4B</i>	3.31	6.25	<i>INS</i>	82,722.95	548,069.76
<i>ATG4C</i>	4.68	-1.95	<i>IRGM</i>	21.35	8.08
<i>ATG4D</i>	-2.08	-3.52	<i>LAMP1</i>	4.30	2.09
<i>ATG5</i>	2.36	1.27	<i>MAP1LC3A</i>	26.83	12.41
<i>ATG7</i>	-1.01	-1.17	<i>MAP1LC3B</i>	9.62	15.71
<i>ATG9A</i>	14.99	44.14	<i>MAPK14</i>	6.80	5.63
<i>ATG9B</i>	1.72	1.61	<i>MAPK8</i>	9.69	3.26
<i>BAD</i>	6.80	5.22	<i>MTOR</i>	432.33	746.50
<i>BAK1</i>	-1.46	-1.07	<i>NFKB1</i>	3.93	1.35
<i>BAX</i>	-1.19	1.48	<i>NPC1</i>	-1.41	-3.65
<i>BCL2</i>	1.97	1.56	<i>PIK3C3</i>	-1.99	-13.60
<i>BCL2L1</i>	17,755.77	-2.42	<i>PIK3CG</i>	15.10	110.97
<i>BECN1</i>	-2.21	-4.49	<i>PIK3R4</i>	3.17	11.58
<i>BID</i>	3.62	10.59	<i>PRKAA1</i>	-3.72	-3.15
<i>BNIP3</i>	-1.25	71.70	<i>PTEN</i>	14.18	2.47
<i>CASP3</i>	8.85	19.75	<i>RAB24</i>	-2.47	-2.63
<i>CASP8</i>	18.97	30.36	<i>RB1</i>	84.80	159.12
<i>CDKN1B</i>	2.44	4.58	<i>RGS19</i>	7.60	1.44
<i>CDKN2A</i>	15.31	15.82	<i>RPS6KB1</i>	2.36	1.41
<i>CLN3</i>	2.36	3.19	<i>SNCA</i>	15.96	56.65
<i>CTSB</i>	547.23	5382.27	<i>SQSTM1</i>	1.16	1.26
<i>CTSD</i>	10.10	14.76	<i>TGFB1</i>	3.62	8.90
<i>CTSS</i>	1.95	3.59	<i>TGM2</i>	2.61	-1.38
<i>CXCR4</i>	-2.05	-3.47	<i>TMEM74</i>	3.13	17.68
<i>DAPK1</i>	-1.48	-3.62	<i>TNF</i>	55.56	80.11
<i>DRAM1</i>	51.84	88.28	<i>TNFSF10</i>	8.43	6.70
<i>DRAM2</i>	-2.61	-8.73	<i>TP53</i>	6.44	9.03
<i>EIF2AK3</i>	-1.05	-2.40	<i>ULK1</i>	732.15	767.49
<i>EIF4G1</i>	3.96	38.43	<i>ULK2</i>	27.02	12.50
<i>ESR1</i>	18.08	28.92	<i>UVRAG</i>	11,315.40	41,591.47
<i>FADD</i>	6.17	2.90	<i>WIPI1</i>	32.36	68.31
<i>FAS</i>	1.24	-1.22	<i>ACTB</i>	-1.55	-1.99
<i>GAA</i>	1.44	1.44	<i>B2M</i>	-1.05	-3.09
<i>GABARAP</i>	1.26	2.49	<i>GAPDH</i>	-4.61	-1.09
<i>GABARAPL1</i>	1.51	1.65	<i>HPRT1</i>	4.91	2.78
			<i>RPLP0</i>	1.53	2.42

Fold-change values in doses of 40 and 120 mM of MTF were calculated using the  $2^{-\Delta\Delta Ct}$  formula and normalized to the values in the control group. Differences in expression more than twofold were accepted as the cut-off value. Values greater than 2 are indicated in red, and fold-regulation values less than -2 are indicated in green

genes facilitating the fusion of autophagosomes with lysosomes. The expression of genes such as DRAM1(51.84-fold and 88.28-fold) and LAMP1(4.30-fold and 2.09-fold) was increased in 40 and 120 mM MTF groups while the expression of GABARAP and NPC1 (-3.65-fold) was altered only in CRC tumoroids exposed to 120 mM MTF. Genes related to ubiquitination of autophagy flux such as ATG3 and HDAC6 (5.60-fold and 7.03-fold) were upregulated in 40 and 120 mM MTF groups.

We noted that 40 and 120 mM MTF changed the expression of ATG12, ATG5, BECN1, AKT1 (4.33-fold and 6.16-fold), APP (26.46-fold and 77.92-fold), BAD (6.80-fold and 5.22-fold), BID (3.62-fold and 10.59-fold), CASP3 (8.85-fold and 19.75-fold), CASP8 (18.97-fold and 30.36), CDKN1B (2.44-fold and 4.58), CDKN2A (15.31-fold and 15.82-fold), CLN3 (2.36-fold and 3.19-fold), CTSB (547.23-fold and 5382.27-fold), DRAM1(51.84-fold and 88.28-fold), FADD (6.17-fold and 2.90-fold), HTT (sixfold and 4.84-fold), INS(82,722.95-fold and 548,069.76), MAPK8 (9.69-fold and 3.26-fold) (JNK1), MTOR (432.33-fold and 746.50-fold), PIK3CG (15.10-fold and 110.97-fold), PTEN (14.18-fold and 2.47-fold), SNCA (15.96-fold and 56.65-fold), TGFB1(3.62-fold and 8.90-fold), TNF(55.56-fold and 80.11-fold), TNFSF10 (8.43-fold and 6.70-fold), TP53 (6.44-fold and 9.03-fold), IFNG (243,911.80-fold and -2.42-fold), BCL2L1 (17,755.77-fold and -2.42-fold), IGF1 (2.69-fold and -5.05-fold), CXCR4 (-2.05-fold and -3.47-fold), PRKAA1 (-3.72-fold and -3.15-fold) are touted as co-regulators of apoptosis and autophagy signaling transduction pathways. In this signaling transduction pathway, NFKB1 (3.93-fold), and TGM2 (2.61-fold) were up-regulated in the presence of

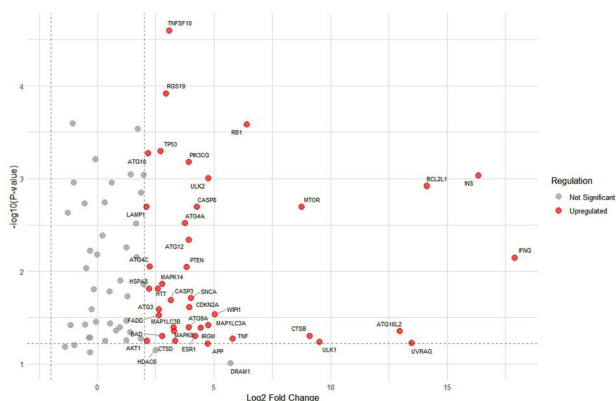
40 mM MTF. The expression of genes such as BNIP3 (71.70-fold), HDAC1 (256.71-fold), DAPK1 (-3.62-fold), and EIF2AK3 (-2.40), were down-regulated in CRC tumoroids when treated with 120 mM MTF.

The transcription of genes related to intracellular signals like CTSD (10.10-fold and 14.76-fold), EIF4G1 (3.96-fold and 38.43-fold), ESR1 (18.08-fold and 28.92-fold), MAPK14 (6.80-fold and 5.63-fold), PIK3R4 (3.17-fold and 11.58-fold), TMEM74 (3.13-fold and 17.68-fold), ULK2 (27.02-fold and 12.50-fold), UVRAG (11,315.4-fold and 41,591.47-fold) was also stimulated. Meanwhile, DRAM2 (-2.61-fold and -8.73-fold) was inhibited in 40 and 120 mM MTF groups compared to the control group. Changes were achieved after treatment with MTF for genes RPS6KB1 (2.36-fold) in 40 mM MTF group and CTSS (3.59-fold), HGS (-72,014.51-fold), and PIK3C3 (-13.60-fold) in 120 mM MTF treated CRC tumoroids. Genes associated with the cell cycles such as CDKN1B, CDKN2A, IFNG, PTEN, TGFB1, TP53, and RB1 (84.80-fold and 159.12-fold) were up-regulated after the modulation of autophagy using 40 and 120 mM MTF. The expression of mediators associated with intracellular pathogens such as IFNG, EIF2AK3, and LAMP1 was also altered. Chaperone-mediated autophagy (CMA) mediators, especially HSPA8, were stimulated (4.65-fold and 2.94-fold) in both the 40 and 120 mM MTF groups, and HSP90AA1 was highly up-regulated (531.53-fold) in the CRC tumoroids treated with 120 mM MTF.

**MTF altered the integrity of CRC tumoroids**

Using H & E staining, it was noted that the central zone of control CRC tumoroids contains several necrotic cells

MTF 40 mM



MTF 120 mM

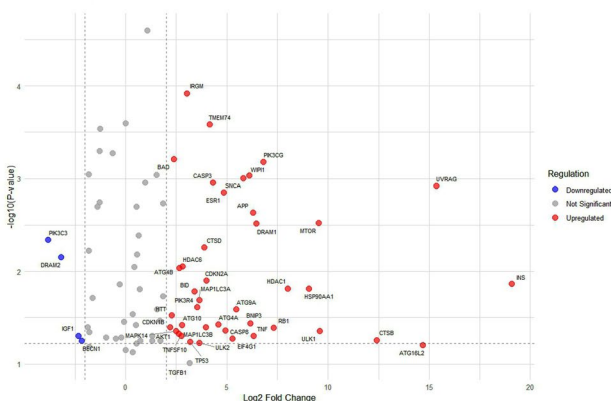


**Fig. 3** Volcano plots indicate up-regulated and down-regulated genes generated in RStudio. The expressed genes are plotted based on the log2 fold change values in MTF 40 mM and MTF 120 mM groups. Red indicates upregulated genes, blue indicates downregulated genes, and gray represents statistically non-significant gene expression

with fragmented nuclei (Fig. 4A). Some cells with intracellular vacuoles were also evident in this region, indicating a typical hypoxic central zone. Bright-field images indicated the existence of numerous flattened cells at the external surface of CRC tumoroids. In the 40 mM MTF group, the number of necrotic (pyknotic nuclei) and apoptotic (subnuclear distribution of condensed chromatin) was also increased (Fig. 4A). In contrast to these changes, the integrity of 120 mM MTF-treated CRC tumoroids was completely lost and numerous apoptotic cells with marginated and condensed chromatin can be observed. Of note, the remanent of isolated tumoroid cells with spindle-shaped morphologies and intercellular fibers was also detected in the group that received 120 mM MTF. These features indicate that increasing

doses of MTF can affect the integrity of CRC tumoroids *in vitro*.

#### MTF influenced the proliferation rate of cells within CRC tumoroids

Using IF staining, it was shown that numerous green-colored Ki-67<sup>+</sup> cells are distributed in the structure of CRC tumoroids (Fig. 4B). These features indicated that CRC tumoroids harbor cells with the proliferation capacity. Notably, the number of Ki-67<sup>+</sup> cells was reduced in tumoroids that received 40 mM MTF while in the MTF 120 mM group, only the remaining cells expressed Ki-67 factor. These data indicated that MTF had the potential to influence the proliferation rate in human CRC tumoroids via changing protein levels of Ki-67 in a dose-dependent

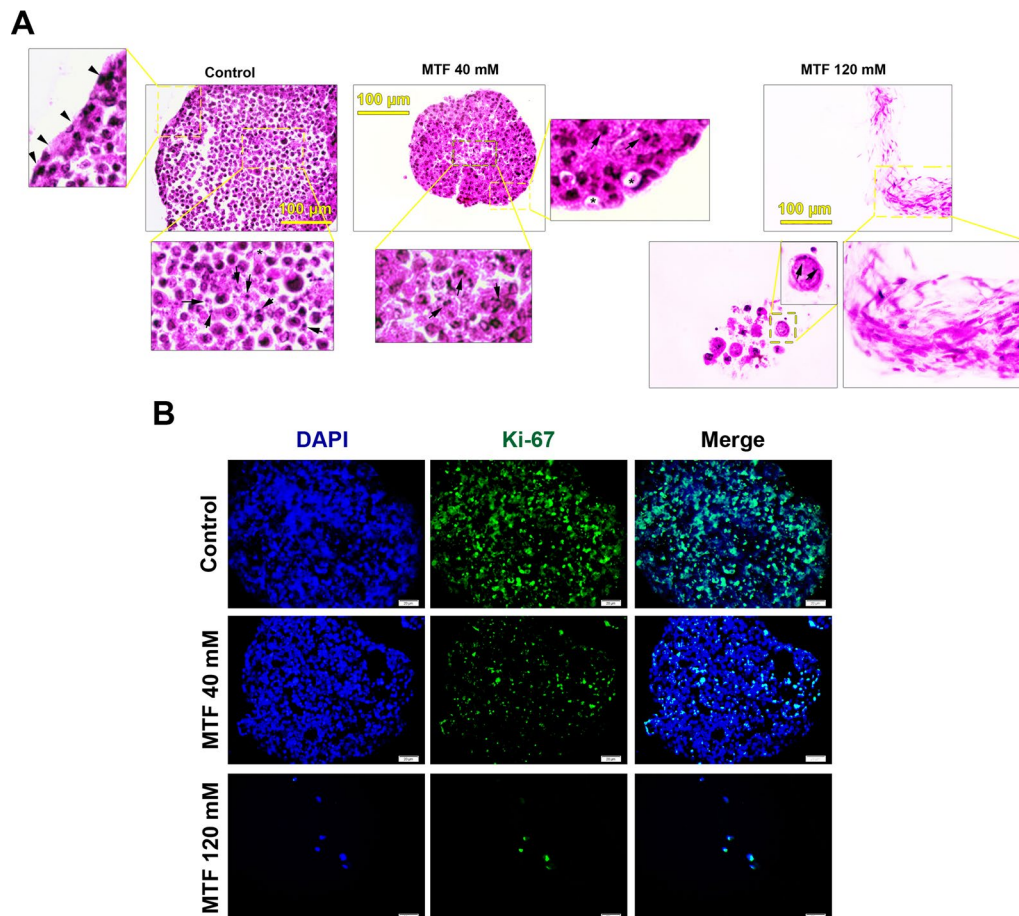


**Fig. 4** H & E staining of CRC tumoroids exposed to 40 and 120 mM MTF for 72 h (A). MTF treatment can lead to the disintegration of cells within the CRC tumoroids in which the number of pyknotic cells (black arrows; 40 mM MTF groups), and swollen cells (asterisks) were increased. Treatment of CRC tumoroids with 120 mM MTF led to an increase of apoptotic cells with marginated chromatin appearance (black arrows) and the existence of spindle-shaped cells. In the control group, central necrotic cells can be detected. Peripheral flattened cells located at the external surface of tumoroids (arrowheads) can be visualized in bright-field images. Immunofluorescence staining of Ki-67<sup>+</sup> cells (B). Data showed that the number of green-colored Ki-67<sup>+</sup> cells with proliferation potential was decreased in the MTF-treated CRC tumoroids. These changes were more evident with the increase of MTF doses from 40 to 120 mM

manner in which the higher doses (120 MTF) can efficiently inhibit the Ki-67 factor and thus proliferation rate.

## Discussion

The present study aimed to evaluate the possible tumoricidal properties of MTF on human CRC tumoroids consisting of HT-29, HFFF2 cells, and HUVECs in vitro. The development and application of 3D culture systems such as organoids with dense cell-to-cell interactions have been extensively used in in vitro settings for mimicking the real tumor niche [32]. Here, the bright-field microscopic images revealed a dense and hypoxic inner central dark zone with numerous necrotic and apoptotic cells. The existence of a hypoxic central region is crucial in solid tumor masses inside the body because of the rapid dynamic growth of cells and depletion of oxygen, glycolytic activity, and acidic pH [33]. These features led to an increase of hypoxia-inducible factor 1 alpha (HIF-1 $\alpha$ ) and activation of several resistance mechanisms such as aldehyde dehydrogenase (ADH), etc. in cells exposed to the proximity of the hypoxic zone [33]. In the paracortical zone, the layer located between the central zone and peripheral layer, a dense cell population was achieved which is enclosed by outer highly proliferative cells. It is believed that these structures can successfully mimic the in vivo-like tumor mass structure.

LDH release assay indicated the lack of MTF cytotoxic effects used at the range between 20 to 1000  $\mu$ M related to the control CRC tumoroids. In several 2D culture systems, lower concentrations of MTF have been examined in various tumor cells in in vitro conditions with prominent tumoricidal properties [34, 35]. Higher doses of MTF used in the current study were not effective in promoting tumoricidal effects on CRC tumoroids. Based on the LDH release assay, 40 and 120 mM MTF doses were selected and used for subsequent analyses. According to our data, the exposure of CRC tumoroids to 40 mM MTF led to the increase of tumoroids diameter while these values were relatively similar in control and 120 mM MTF-treated CRC tumoroids. In the 120 mM MTF groups, several sloughed single cells can be detected on the surface of culture plates indicating the possible cytotoxic properties of a high dose of MTF on proliferative cells located at the outermost tumoroid layer. Along with these data, IF staining indicated the reduction of Ki-67<sup>+</sup> cells with the proliferation capacity in the MTF-treated groups especially in the 120 mM MTF group. It has been indicated that MTF can inhibit mitochondrial oxidation via the suppression of NADH-coenzyme Q oxidoreductase and reduction of  $\Delta\Psi$ , leading to tumoricidal effects [36]. Such effects can reduce the activity of enzymes belonging to the tricarboxylic cycle and inhibit cell growth in the tumoroid system, especially in the periphery zone.

The increase of the AMP/ATP ratio provokes the activity of AMPK kinase, inhibits mTOR, and activates several signaling pathways especially autophagy response [36, 37]. Thus, it is postulated that the lack of significant differences in terms of tumoroid diameter between the control and 120 mM MTF-treated CRC tumoroids is related to the existence of a compact cell layer in control tumoroids and sloughing of dead cells from the external surface of 120 mM treated-MTF tumoroids. Along with these descriptions, numerous single disintegrated cells were detected in the bottom surface of culture plates in the 120 mM MTF group. Based on previously conducted experiments, MTF can exhibit strong synergistic tumoricidal properties and tumor suppression in combination with chemotherapeutics. For instance, MTF with different chemotherapeutics can efficiently reduce the phosphorylation of Akt, and control the Akt/mTOR signaling axis [38]. It is believed that MTF can reduce glucose levels which can affect the dynamic tumor cell growth and then sensitize these cells to various chemotherapeutics especially when applied before the chemotherapy [39]. For example, the induction of autophagic response sensitizes SKOV3/DDP ovarian cancer cells against cisplatin [39]. In this regard, recent clinical trials have successfully used the combined regime of MTF with different chemotherapeutics, *i.e.*, carboplatin or paclitaxel in cancer patients [40]. The co-administration of MTF with chemotherapeutics increases the survival rate in colorectal cancer patients with improved pathological complete response [41]. Despite these achievements, determining the optimal doses of MTF should be done in cancer patients to reduce the possible side effects.

During the last decades, autophagy has become a promising signaling pathway target for cancer therapy. However, there are controversial debates about the effects of autophagy on cancer cell survival or suppression [42, 43]. As mentioned before, MTF can stimulate the autophagic response in different cancer types, such as colon, endometrial cancer cells, and melanoma, and the application of this drug is approved by the FDA for metabolic disorders [43–45]. Novel cell culture techniques are valid analytic tools for monitoring the efficiency of therapeutic drugs and the conduction of personalized medicine [46]. Here, we indicated that protein levels of Becnin-1 were slightly induced in 40 and 120 mM MTF-treated groups. Despite the increase of total LC3 content in tumoroids in the presence of 120 mM MTF, the lipidation and conversion of LC3-I to LC3-II were reduced in the presence of 120 mM MTF but not 40 mM MTF group, indicating the inhibition of autophagic flux at higher MT doses. Along with these changes, the intracellular p62 levels were reduced in the 120 mM MTF-treated group. The reduction of p62 levels can be

associated with reduced formation of ubiquitin<sup>+</sup> aggregates, and impaired or overactivated autophagy response [47–49]. Using autophagy PCR array analysis, we found changes in the expression of several autophagy mediators. Genes belonging to different autophagy signal transduction pathways such as autophagic vacuole formation, vacuole targeting protein transport, autophagosome-lysosome linkage ubiquitination proteases, co-regulators of autophagy & apoptosis, co-regulators of autophagy & the cell cycle, autophagy induction by intracellular pathogens, autophagy in response to other intracellular signals, and chaperone-mediated autophagy were monitored (Supplementary Table 1). Irrespective of the up-regulation, and down-regulation of several autophagy-related genes, PCR array analysis indicated the significant changes in the expression of genes related to co-regulators of autophagy & apoptosis, co-regulators of autophagy signaling transduction pathway.

It was suggested that apoptosis can control cell death and is a valid therapeutic target for CRCs. It is hypothesized that concurrent stimulation of apoptosis and autophagy can exert prominent oncostatic effects after being exposed to chemotherapeutics [50]. Based on previous studies, there is an intricate reciprocal interaction between the autophagy and apoptosis signaling pathways by engaging a diverse array of genes with promoting, synergistic, and antagonistic effects [51]. Here, we found that the expression of different shared genes between autophagy and apoptosis such as BAD, BID, CASP3, CASP8, CDKN1B, DRAM1, FADD, PTEN, TGFB1, TNF, TNFSF10, TP53, PRKAA1, CXCR4, mTOR, ATG12, ATG5, BECN1, and AKT1 were significantly changed compared to the control CRC tumoroids. Along with the present data, it has been declared that MTF can induce both apoptosis and autophagic response in tumor cells [52–55]. Concomitant with the activation of several anti-apoptotic genes, the expression of certain gene types such as BCL2L1 was highly induced in 40 mM MF-treated CRC tumoroids while 120 mM MTF can strongly suppress the expression of this gene [56]. These data indicate that lower concentration of MTF, not only, cannot activate certain pro-apoptotic genes, but also increases distinct anti-apoptotic factors that can lead to the activation of several resistance mechanisms. Histological examination indicated the existence of numerous apoptotic, necrotic cells and degenerated swollen cells in 40 mM MTF-treated groups. These features were more evident in 120 mM MTF-treated CRC tumoroids. Unlike the 40 mM MTF group, the number of spindle-shaped cells was increased which can be related to certain cellular mechanisms in distinct cell lineages such as fibroblasts after interaction with the tumor cells even in the presence of MTF [57]. One reason for the presence of fibroblast-like

cells is possibly related to the up-regulation of the TGF- $\beta$  gene as indicated in the PCR array panel. However, we did not use any specific markers to follow up on certain cell phenotypes within the CRC tumoroids after being exposed to MTF. Based on the previous data, different underlying mechanisms have been proposed for the inhibition of CRC cells after being exposed to MTF. It was suggested that MTF can inhibit the activity of INHBA, a TGF- $\beta$  signaling pathway ligand, in CRC cells, leading to the regulation of the PI3K/Akt pathway, reduction of cyclinD1, and tumor cell arrest [58]. Similar to the current experiment, previous data indicated that MTF can stimulate several cell damage mechanisms such as apoptosis and autophagy in CRC cells in a dose-dependent manner. The activation of AF-1, Map-LC3, Caspase-3, and PARP, and reduction of NRF-2 coincided with NF- $\kappa$ B stimulation can foster CRC cell injury. Likewise, the reduction of resistant cancer stem cells (CD133<sup>+</sup>/CD44<sup>+</sup> subpopulation) has been also reported in CRC cells after incubation with MTF [59].

## Conclusions

The present study shed valid data about the tumoricidal properties of MTF in CRC tumoroids with the potential to relatively recapitulate tumor-like parenchyma human body. Data confirmed that MTF had the potential to stimulate an excessive autophagic response, and activation of apoptosis-related genes, with simultaneous inhibition of proliferation (Ki-67<sup>+</sup> cells), and increase of necrotic changes, leading to the disintegration of CRC tumoroids. These effects were heightened in the presence of higher doses of MTF.

Although the tumoroid systems provide high-throughput theranostic screening platforms much better compared to the 2D culture systems, the current data face some potential limitations that should be addressed using different studies. The current system cannot completely mimic the real cell-to-ECM and cell-to-cell interaction within the tumor parenchyma. Different ECM components, including proteins, carbohydrates, and other macromolecules exist within the tumor stroma in various ratios [60], while only 2.5% methylcellulose was used as a supporting matrix to develop human 3D colon cancer tumoroids. Due to differences in tumor cell subpopulations with various phenotypes and interstitial ECM entities, and the presence of immune cells, and other non-tumor cells, the obtained data from the present experiment could not be completely applicable to all tumor types. However, the current technology enables us to provide a valid personalized theranostic platform in the clinical setting for achieving better therapeutic outcomes and circumventing the issues associated with cancer heterogeneity.

Of note, patient-derived tumoroids possess relatively donor tissue microstructure and evaluate the efficiency of applied therapeutic protocols in *in vivo* conditions [61]. Of note, the lack of standard protocols for tumoroid formation and expansion, genetic variations, and different tumor cell behavior can lead to difficulty in the interpretation of data [62]. By advancing 3D tumor modeling, it is possible to develop valid and accurate 3D patient avatars for selecting suitable therapeutic protocols in the clinical setting.

## Supplementary Information

The online version contains supplementary material available at <https://doi.org/10.1186/s13287-025-04174-z>.

Additional file1.  
Additional file2.  
Additional file3.  
Additional file4.  
Additional file5.  
Additional file6.  
Additional file7.  
Additional file8.

## Acknowledgements

Authors wish to thank the personnel of the Infectious and Tropical Diseases Research Center for their help and guidance.

## Author contributions

R.S., S.H., M.S.M., F.S., A.B., and A.R.N.Z. were involved in cell culture techniques and development of CRC tumoroids and preparing the draft. Ç.B.A., M.M., L.S.T., and M.S.T. performed PCR array analysis and interpretation. R.R. supervised the study and edited the draft.

## Funding

This study was supported by a grant (67863) from Tabriz University of Medical Sciences. The funding body played no role in the design of the study and collection, analysis, and interpretation of data and in writing the manuscript.

## Data Availability

All data underlying the results are available as part of the article.

## Declarations

### Ethics approval and consent to participate

No human and/or animal samples were used in this study. The study was registered as titled "The effect of metformin on induction of autophagy in tumoroid structures of colorectal cancer" under an approval code of IR.TBZMED.VCR.REC.1401.011 from Research Ethics Committees of Vice-Chancellor in Research Affairs—Tabriz University of Medical Sciences on 2022–04-04.

### Consent for publication

Human HT-29 cells (NCBI code: C154), HFFF2 cells (NCBI code: C163), and HUVECs (NCBI code: C554) were purchased from cell line collections of the National Cell Bank of Iran (NCBI). URL: <https://fa1.pasteur.ac.ir/GCellBankSearch.aspx>.

### Competing interests

No potential conflict of interest was reported by the authors.

## Author details

<sup>1</sup>Infectious and Tropical Diseases Research Center, Tabriz University of Medical Sciences, Tabriz, Iran. <sup>2</sup>Department of Medical Genetics, Faculty of Medicine, Tabriz University of Medical Sciences, Tabriz, Iran. <sup>3</sup>Department of Medical Biology, Faculty of Medicine, Ege University, Izmir, Turkey. <sup>4</sup>Department of Clinical Biochemistry and Laboratory Medicine, School of Medicine, Tabriz University of Medical Sciences, Tabriz, Iran. <sup>5</sup>Stem Cell Research Center, Tabriz University of Medical Sciences, Tabriz, Iran. <sup>6</sup>Department of Applied Cell Sciences, Faculty of Advanced Medical Sciences, Tabriz University of Medical Sciences, Tabriz, Iran.

Received: 20 May 2024 Accepted: 23 January 2025

Published online: 04 February 2025

## References

- Sawicki T, et al. A review of colorectal cancer in terms of epidemiology, risk factors, development, symptoms and diagnosis. *Cancers*. 2021;13(9):2025.
- Krasteva N, Georgieva M. Promising therapeutic strategies for colorectal cancer treatment based on nanomaterials. *Pharmaceutics*. 2022;14(6):1213.
- Narmi MT, et al. Melatonin blunted the angiogenic activity in 3D colon cancer tumoroids by the reduction of endocan. *Cancer Cell Int*. 2023;23(1):118.
- Kapalczyńska M, et al. 2D and 3D cell cultures—a comparison of different types of cancer cell cultures. *Arch Med Sci*. 2018;14(4):910–9.
- Loessner D, et al. Bioengineered 3D platform to explore cell–ECM interactions and drug resistance of epithelial ovarian cancer cells. *Biomaterials*. 2010;31(32):8494–506.
- Abdolahinia ED, et al. Enhanced penetration and cytotoxicity of metformin and collagenase conjugated gold nanoparticles in breast cancer spheroids. *Life Sci*. 2019;231: 116545.
- Scalise M, et al. From spheroids to organoids: the next generation of model systems of human cardiac regeneration in a dish. *Int J Mol Sci*. 2021;22(24):13180.
- Yousafzai MS, Hammer JA. Using Biosensors to Study Organoids, Spheroids and Organs-on-a-Chip: A Mechanobiology Perspective. *Biosensors*. 2023;13(10):905.
- Zhang R, et al. Development and application of patient-derived cancer organoids in clinical management of gastrointestinal cancer: a state-of-the-art review. *Front Oncol*. 2021;11: 716339.
- Weeber F, et al. Preserved genetic diversity in organoids cultured from biopsies of human colorectal cancer metastases. *Proc Natl Acad Sci U S A*. 2015;112(43):13308–11.
- Árnadóttir SS, et al. Characterization of genetic intratumor heterogeneity in colorectal cancer and matching patient-derived spheroid cultures. *Mol Oncol*. 2018;12(1):132–47.
- Molla A, Couvet M, Coll JL. Unsuccessful mitosis in multicellular tumour spheroids. *Oncotarget*. 2017;8(17):28769–84.
- Liu Q, et al. Cancer cells growing on perfused 3D collagen model produced higher reactive oxygen species level and were more resistant to cisplatin compared to the 2D model. *J Appl Biomater Funct Mater*. 2018;16(3):144–50.
- Murrow L, Debnath J. Autophagy as a stress-response and quality-control mechanism: implications for cell injury and human disease. *Annu Rev Pathol*. 2013;8:105–37.
- Gentile D, Esposito M, Grumati P. Metabolic adaption of cancer cells toward autophagy: Is there a role for ER-phagy? *Front Mol Biosci*. 2022;9: 930223.
- Cao Y, et al. Autophagy and its role in gastric cancer. *Clin Chim Acta*. 2019;489:10–20.
- Gozuacik D, Kimchi A. Autophagy and cell death. *Curr Top Dev Biol*. 2007;78:217–45.
- Chavez-Dominguez R, et al. The Double-Edge Sword of Autophagy in Cancer: From Tumor Suppression to Pro-tumor Activity. *Front Oncol*. 2020;10: 578418.

19. Yu H, et al. The potential effect of metformin on cancer: an umbrella review. *Front Endocrinol.* 2019;10:617.
20. Cardel M, et al. Long-term use of metformin and colorectal cancer risk in type II diabetics: a population-based case-control study. *Cancer Med.* 2014;3(5):1458–66.
21. Lee MS, et al. Type 2 diabetes increases and metformin reduces total, colorectal, liver and pancreatic cancer incidences in Taiwanese: a representative population prospective cohort study of 800,000 individuals. *BMC Cancer.* 2011;11:20.
22. Sehdev A, et al. Metformin for primary colorectal cancer prevention in patients with diabetes: a case-control study in a US population. *Cancer.* 2015;121(7):1071–8.
23. Tseng CH. Diabetes, metformin use, and colon cancer: a population-based cohort study in Taiwan. *Eur J Endocrinol.* 2012;167(3):409–16.
24. Zhang ZJ, et al. Reduced risk of colorectal cancer with metformin therapy in patients with type 2 diabetes: a meta-analysis. *Diabetes Care.* 2011;34(10):2323–8.
25. Ferrara A, et al. Cohort study of pioglitazone and cancer incidence in patients with diabetes. *Diabetes Care.* 2011;34(4):923–9.
26. Kowall B, et al. No reduced risk of overall, colorectal, lung, breast, and prostate cancer with metformin therapy in diabetic patients: database analyses from Germany and the UK. *Pharmacoepidemiol Drug Saf.* 2015;24(8):865–74.
27. Lin CM, et al. Association between Gastroenterological Malignancy and Diabetes Mellitus and Anti-Diabetic Therapy: A Nationwide, Population-Based Cohort Study. *PLoS ONE.* 2015;10(5):e0125421.
28. Smiechowski B, et al. The use of metformin and colorectal cancer incidence in patients with type II diabetes mellitus. *Cancer Epidemiol Biomarkers Prev.* 2013;22(10):1877–83.
29. Bodmer M, et al. Metformin does not alter the risk of lung cancer: a case-control analysis. *Lung Cancer.* 2012;78(2):133–7.
30. Knapen LM, et al. Use of biguanides and the risk of colorectal cancer: a register-based cohort study. *Curr Drug Saf.* 2013;8(5):349–56.
31. Yudhani, R.D., et al., *Metformin Modulates Cyclin D1 and P53 Expression to Inhibit Cell Proliferation and to Induce Apoptosis in Cervical Cancer Cell Lines.* 2019. 20(6): p. 1667–1673.
32. Xu H, et al. Tumor organoids: applications in cancer modeling and potentials in precision medicine. 2022;15(1):58.
33. Emami Nejad A, et al. The role of hypoxia in the tumor microenvironment and development of cancer stem cell: a novel approach to developing treatment. *Cancer Cell Int.* 2021;21(1):62.
34. Szymczak-Pajor, I., et al. *Metformin Induces Apoptosis in Human Pancreatic Cancer (PC) Cells Accompanied by Changes in the Levels of Histone Acetyltransferases (Particularly, p300/CBP-Associated Factor (PCAF) Protein Levels).* *Pharmaceuticals*, 2023. 16. <https://doi.org/10.3390/ph16010115>.
35. Hsieh Li S-M, et al. Metformin causes cancer cell death through down-regulation of p53-dependent differentiated embryo chondrocyte 1. *J Biomed Sci.* 2018;25(1):81.
36. Hua Y, et al. Metformin and cancer hallmarks: shedding new lights on therapeutic repurposing. *J Transl Med.* 2023;21(1):403.
37. Kim YC, Guan KL. mTOR: a pharmacologic target for autophagy regulation. *J Clin Invest.* 2015;125(1):25–32.
38. Wen KC, et al. Neoadjuvant metformin added to conventional chemotherapy synergizes anti-proliferative effects in ovarian cancer. *J Ovarian Res.* 2020;13(1):95.
39. Yang C, et al. Metformin improves the sensitivity of ovarian cancer cells to chemotherapeutic agents. *Oncol Lett.* 2019;18(3):2404–11.
40. Zhu L, et al. Metformin as anticancer agent and adjuvant in cancer combination therapy: Current progress and future prospect. *Translational Oncology.* 2024;44: 101945.
41. Skinner HD, et al. Metformin use and improved response to therapy in rectal cancer. *Cancer Med.* 2013;2(1):99–107.
42. Amaravadi RK, et al. Autophagy inhibition enhances therapy-induced apoptosis in a Myc-induced model of lymphoma. *J Clin Invest.* 2007;117(2):326–36.
43. Buzzai M, et al. Systemic treatment with the antidiabetic drug metformin selectively impairs p53-deficient tumor cell growth. *Cancer Res.* 2007;67(14):6745–52.
44. Takahashi A, et al. Metformin impairs growth of endometrial cancer cells via cell cycle arrest and concomitant autophagy and apoptosis. *Cancer Cell Int.* 2014;14:53.
45. Tomic T, et al. Metformin inhibits melanoma development through autophagy and apoptosis mechanisms. *Cell Death Dis.* 2011;2(9): e199.
46. Dutta D, Heo I, Clevers H. Disease Modeling in Stem Cell-Derived 3D Organoid Systems. *Trends Mol Med.* 2017;23(5):393–410.
47. Schläfli AM, et al. Prognostic value of the autophagy markers LC3 and p62/SQSTM1 in early-stage non-small cell lung cancer. *Oncotarget.* 2016;7(26):39544–55.
48. Abrar, F., et al., *Reduced S-acylation of SQSTM1/p62 in Huntington disease is associated with impaired autophagy.* *bioRxiv*, 2023: p. 2023.10.11.561600.
49. Liu WJ, et al. p62 links the autophagy pathway and the ubiquitin–proteasome system upon ubiquitinated protein degradation. *Cell Mol Biol Lett.* 2016;21(1):29.
50. Qian H-R, et al. Interplay between apoptosis and autophagy in colorectal cancer. *Oncotarget.* 2017;8(37):62759.
51. Su, M., Y. Mei, and S. Sinha, *Role of the crosstalk between autophagy and apoptosis in cancer.* *Journal of oncology*, 2013. 2013.
52. Buzzai M, et al. Systemic treatment with the antidiabetic drug metformin selectively impairs p53-deficient tumor cell growth. *Can Res.* 2007;67(14):6745–52.
53. Liu B, et al. Metformin induces unique biological and molecular responses in triple negative breast cancer cells. *Cell Cycle.* 2009;8(13):2031–40.
54. Wang L-W, et al. Metformin induces apoptosis of pancreatic cancer cells. *World J Gastroenterol.* 2008;14(47):7192.
55. Kourelis TV, Siegel RD. Metformin and cancer: new applications for an old drug. *Med Oncol.* 2012;29:1314–27.
56. Lee A-J, Liao H-J, Hong J-R. Overexpression of Bcl2 and Bcl2L1 can suppress betanodavirus-induced type III cell death and autophagy induction in GF-1 cells. *Symmetry.* 2022;14(2):360.
57. De, P. and J. Aske, *Cancer-Associated Fibroblast Functions as a Road-Block in Cancer Therapy.* 2021. 13(20).
58. Xiao Q, et al. Metformin suppresses the growth of colorectal cancer by targeting INHBA to inhibit TGF- $\beta$ /PI3K/AKT signaling transduction. *Cell Death Dis.* 2022;13(3):202.
59. Kamarudin MNA, et al. Metformin in colorectal cancer: molecular mechanism, preclinical and clinical aspects. *J Exp Clin Cancer Res.* 2019;38(1):491.
60. Habanjar O, et al. 3D cell culture systems: tumor application, advantages, and disadvantages. *Int J Mol Sci.* 2021;22(22):12200.
61. Sato T, et al. Single Lgr5 stem cells build crypt-villus structures in vitro without a mesenchymal niche. *Nature.* 2009;459(7244):262–5.
62. Soto-Gamez A, et al. Organoid-based personalized medicine: from tumor outcome prediction to autologous transplantation. *Stem Cells.* 2024;42(6):499–508.

## Publisher's Note

Springer Nature remains neutral with regard to jurisdictional claims in published maps and institutional affiliations.